

Hybrid Tracking Loop Architectures for the Galileo E5 Signal

Nagaraj C Shivaramaiah, Andrew G. Dempster and Chris Rizos
School of Surveying & Spatial Information Systems
University of New South Wales, Sydney 2052, Australia

BIOGRAPHY

Nagaraj C Shivaramaiah is currently a doctoral student within the GNSS receiver design group in the School of Surveying & Spatial Information Systems at the University of New South Wales (UNSW), Australia. He has a Masters degree in Electronics Design and Technology from the Indian Institute of Science, Bangalore, India. He has been involved in GNSS related research since the late 1990s. Prior to joining UNSW, he worked at Freescale Semiconductors, Bangalore and Accord Software and Systems, Bangalore. His research interests include GNSS receiver design, baseband signal processing, baseband ASIC design, embedded and reconfigurable hardware design and software defined radios. He is a student member of the IEEE and of the U.S. Institute of Navigation.

Andrew G Dempster has a BE (1984) and MEngSc (1992) in Electrical Engineering from the UNSW and PhD (1995) in Signal Processing from Cambridge University, UK. He has worked for STC in Sydney as a Telecommunications Design Engineer, for Auspace Limited in Canberra as a Systems Engineer and Project Manager, and for University of Westminster in London as a Lecturer, Senior Lecturer and Senior Academic. He is currently Director of Research in the School of Surveying and Spatial Information Systems at the UNSW. His current research interests cover satellite navigation receiver design, interference effects, weak-signal GNSS, new positioning technologies, integration of location technologies, and software defined radio.

Prof. Chris Rizos is currently the Head of the School of Surveying & Spatial Information Systems, UNSW. Chris has been researching the technology and applications of GPS since 1985, and established over a decade ago the Satellite Navigation and Positioning group at UNSW, today the largest and best known academic GPS and wireless location technology R&D laboratory in

Australia. Chris is the Vice President of the International Association of Geodesy (IAG), and a member of the Governing Board and Executive of the International GNSS Service (IGS). Chris is a Fellow of the IAG and a Fellow of the Australian Institute of Navigation.

ABSTRACT

Due to their structure, Galileo E5 signals offer a number of ways to synchronise the signal and to demodulate the data. In this paper the authors describe the architectures required, and discuss the pros and cons of several of these methods, for tracking the E5 signal. It is shown that the trade-offs in tracking individual components of the E5 signal can be converted to advantages thereby improving the tracking jitter performance in low signal strength environments.

I. INTRODUCTION

Galileo E5 signals are the most sophisticated signals in the GNSS spectrum employing a special class of Complex Double Binary Offset Carrier (CDBOC) modulations known as AltBOC (Alternate Binary Offset Carrier) modulation. The signal comprises four tiered codes each with chipping rate $f_c = 10.23$ MHz. These are combined with in-phase and quadrature components of specially chosen sub-carrier waveforms of frequency $f_s = 15.345$ MHz, resulting in constant envelope AltBOC(15,10) modulation, which resembles an 8-PSK. Like other offset carrier modulations, AltBOC modulation also splits the spectrum into two halves which are called E5a and E5b. The main lobes of the separated signals occupy a total bandwidth of ~ 51 MHz around the centre frequency of 1191.795 MHz. Unlike other GNSS offset carrier modulations the two lobes each carry two distinct signals. Of the four tiered codes modulated onto the E5 signal, which are referred to as E5a-I, E5a-Q, E5b-I and E5b-Q, only the in-phase signals carry the data; the quadrature-phase signals are pilot signals. The

constant envelope AltBOC scheme generates product signal as a by-product of the modulation which consumes 14.64% of the total power, and hence the four individual codes equally share 21.34% of the received power (a total of 85.36%).

The presence of several parameters in the AltBOC modulation from its four primary codes, four secondary codes, four phases of a sub-carrier, two data components all of which are appropriately mapped onto four signal components, makes the efficient synchronisation of the AltBOC signal an interesting and challenging task. Several strategies for signal acquisition have been discussed in Shivaramaiah and Dempster (2008). A sequential search method to identify the phase of the secondary code has been discussed in Shivaramaiah et. al. (2008). The subsequent step of *tracking* the signal is the topic of this paper.

This paper is organised as follows. Section II describes the principles of the standard tracking architectures applicable to the E5 signal and discusses their advantages and disadvantages. Section III discusses the proposed method of carrier and code tracking. Section IV provides the performance analysis, followed by the conclusions in section V.

II. STANDARD TRACKING ARCHITECTURE FOR THE GALILEO E5 SIGNAL

The received signal at an intermediate frequency (IF) in the case of Galileo E5 AltBOC can be represented as (considering any one satellite) (Kaplan and Hegarty 2006):

$$r_{IF}(t) = \sqrt{2P} \cdot \Re \left[s(t - \tau) \cdot e^{j(\omega_{IF}t + \omega_d t + \phi)} \right] + n(t) \quad (1)$$

where P is the received power, ω_{IF} is the intermediate frequency, ω_d is the Doppler frequency, ϕ is the phase of the received signal, $s(t - \tau)$ is the complex baseband signal with a time delay τ w.r.t. the transmitted signal, and $n(t)$ is the additive white Gaussian noise. The complex baseband signal can be represented as $s(t) = s_c(t) + js_s(t)$. Hence (1) can be written as:

$$r_{IF}(t) = \sqrt{2P} \begin{pmatrix} s_c(t - \tau) \cdot \cos(\omega_0 t + \phi) \\ s_s(t - \tau) \cdot \sin(\omega_0 t + \phi) \end{pmatrix} + n(t) \quad (2)$$

where $\omega_0 = \omega_{IF} + \omega_d$. The cosine and sine components are generated according to the AltBOC modulation scheme described in OS SIS ICD (2008, pp. 5-8).

The receiver front-end typically uses a bandwidth of at least 51 MHz so as to pass the first two main lobes of the signal spectrum. As with the processing methods for the acquisition explained in Shivaramaiah and Dempster (2008) and Dervis et. al. (2007), the signal tracking can also use similar techniques to track the complete E5 AltBOC or any component of the signal. The first method in which the E5a and E5b signals are translated from their centre frequencies to the baseband is called the Side-Band Translation (SBT) method. The local signal is then generated free of sub-carriers. The second method is the Full-band Independent Correlation (FIC) in which the local signal is generated for the required signal component mapped onto the appropriate phase of the sub-carrier. The third method is the 8-PSK-like processing which allows only the complete E5 signal correlation by the use of a look-up table (LUT). With the first two methods, several combinations of signal components are possible with the combination variables being coherent and non-coherent, data and pilot, E5a and E5b.

The received signal is correlated with the locally generated code and carrier with the estimates of the code delay $\hat{\tau}$, carrier frequency and phase $\hat{\omega}_0, \hat{\phi}$.

Fig. 1 shows a generalised tracking architecture for the E5 signal. This architecture holds good for all three methods of processing mentioned in the previous paragraph. The received signal is multiplied with the locally generated carrier $x(t)$ to obtain the baseband signal. For the SBT method,

$$x(t) = x_{SBT}(t) = e^{-j(\hat{\omega}_0 t + \hat{\phi} \pm \omega_s t)} \quad (3)$$

where $\omega_s = 2\pi f_s$ is the sub-carrier angular frequency and the preceding sign depends on whether we are interested in E5a or E5b. For the FIC and 8-PSK methods:

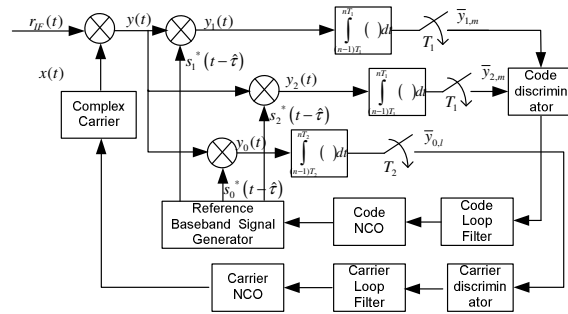


Figure 1 Generalised architecture for the E5 signal tracking

$$x(t) = x_{FIC}(t) = x_{8-PSK}(t) = e^{-j(\hat{\omega}_0 t + \hat{\phi})} \quad (4)$$

The resultant signal $y(t)$ is then multiplied with the reference baseband signal, followed by an integrate and dump circuit and the tracking loop modules. The choice of the baseband reference signal is the differentiating parameter by which additional tracking architectures are possible in addition to the SBT, FIC and 8-PSK methods. In this architecture, a delay-lock tracking is assumed for the code with two time-delayed reference signals $s_1(t-\hat{\tau})$ and $s_2(t-\hat{\tau})$. For the carrier tracking an on-time reference signal is assumed, represented by $s_0(t-\hat{\tau})$. When both the carrier and code tracking loops use the same signal component(s) for the tracking then:

$$\begin{aligned} s_1(t-\hat{\tau}) &= s_0(t-\hat{\tau}-\delta T_c) \\ s_2(t-\hat{\tau}) &= s_0(t-\hat{\tau}+\delta T_c) \end{aligned} \quad (5)$$

where δ is the chip spacing used for the delayed signals from the on-time signal and T_c is the chip duration. Unless otherwise specified we assume this configuration throughout the paper.

Reference signals with the SBT method

Table 1 shows several possibilities of the reference signals with the SBT method. The reference signal $s_r(t-\hat{\tau})$ could be applied to any of the $r=0,1,2$ case.

The parameter $e_r(\cdot)$ is the primary code plus secondary code plus navigation data (for the I components) as defined in OS SIS ICD (2008) and GIOVE-A+B Public SIS ICD (2008). When correlated with $y(t)$, all the reference signals result in a BPSK(10)-like correlation triangle due to the absence of the sub-carrier. Note that the last two reference signals are coherent summation of the data and pilot components. Since the reference signal is generated without the data, there is an ambiguity in deciding the sign of the summation.

Table 1 Possible reference signals with the SBT method

Signal component of interest	Reference baseband signal $s_r(t-\hat{\tau})$
E5a-I (data)	$e_{a-I}(t-\hat{\tau})$
E5a-Q (pilot)	$e_{a-Q}(t-\hat{\tau})$
E5b-I (data)	$e_{b-I}(t-\hat{\tau})$
E5b-Q (pilot)	$e_{b-Q}(t-\hat{\tau})$
E5a	$e_{a-I}(t-\hat{\tau}) \pm j \cdot e_{a-Q}(t-\hat{\tau})$
E5b	$e_{b-I}(t-\hat{\tau}) \pm j \cdot e_{b-Q}(t-\hat{\tau})$

Reference signals with the FIC method

Table 2 shows the possible reference signals using the FIC method. In order to achieve the constant envelope modulation at the transmitter, the sub-carrier is separated into two parts: the sum-sub-carrier and the product-sub-carrier. The sum-sub-carrier $sc_{sum}(t) = sc_s(t) + j \cdot sc_s(t-T_s/4)$ is the major part whose phase is used to modulate the four components of the E5 signal (T_s is the sub-carrier period).

The product-sub-carrier $sc_{prod}(t) = sc_p(t) + j \cdot sc_p(t-T_s/4)$ modulates the product codes. The waveforms sc_s and sc_p are defined in OS SIS ICD (2008). It is possible to incorporate the product codes also into the reference signal. As shown in the Appendix, the product signals are of no advantage for receiver bandwidths less than 100 MHz. Hence we can safely neglect the product signal from inclusion in the reference signal.

Table 2 Possible reference signals with the FIC method

Signal component of interest	Reference baseband signal $s_r(t-\hat{\tau})$
E5a-I (data)	$\frac{1}{2\sqrt{2}} \cdot e_{a-I}(t-\hat{\tau}) \cdot sc_{sum}(t-\hat{\tau})$
E5a-Q (pilot)	$\frac{j}{2\sqrt{2}} \cdot e_{a-Q}(t-\hat{\tau}) \cdot sc_{sum}(t-\hat{\tau})$
E5b-I (data)	$\frac{1}{2\sqrt{2}} \cdot e_{b-I}(t-\hat{\tau}) \cdot sc_{sum}^*(t-\hat{\tau})$
E5b-Q (pilot)	$\frac{j}{2\sqrt{2}} \cdot e_{b-Q}(t-\hat{\tau}) \cdot sc_{sum}^*(t-\hat{\tau})$
E5a	$\frac{1}{2\sqrt{2}} \cdot \left(e_{a-I}(t-\hat{\tau}) \pm j \cdot e_{a-Q}(t-\hat{\tau}) \right) \cdot sc_{sum}(t-\hat{\tau})$
E5b	$\frac{1}{2\sqrt{2}} \cdot \left(e_{b-I}(t-\hat{\tau}) \pm j \cdot e_{b-Q}(t-\hat{\tau}) \right) \cdot sc_{sum}^*(t-\hat{\tau})$
E5p (E5a-Q and E5b-Q)	$\frac{j}{2\sqrt{2}} \cdot e_{a-Q}(t-\hat{\tau}) \cdot sc_{sum}(t-\hat{\tau}) + \frac{j}{2\sqrt{2}} \cdot e_{b-Q}(t-\hat{\tau}) \cdot sc_{sum}^*(t-\hat{\tau})$
E5d (E5a-I and E5b-I)	$\frac{1}{2\sqrt{2}} \cdot e_{a-I}(t-\hat{\tau}) \cdot sc_{sum}(t-\hat{\tau}) \pm \frac{1}{2\sqrt{2}} \cdot e_{b-I}(t-\hat{\tau}) \cdot sc_{sum}^*(t-\hat{\tau})$
E5ab	$\pm \frac{1}{2\sqrt{2}} \cdot \left(e_{a-I}(t-\hat{\tau}) + j \cdot e_{a-Q}(t-\hat{\tau}) \right) \cdot sc_{sum}(t-\hat{\tau}) \pm \frac{1}{2\sqrt{2}} \cdot \left(e_{b-I}(t-\hat{\tau}) + j \cdot e_{b-Q}(t-\hat{\tau}) \right) \cdot sc_{sum}^*(t-\hat{\tau})$

When correlated with $y(t)$, the first six reference signals result in a BPSK(10)-like correlation waveform. The last three reference signals result in a AltBOC(15,10)-like correlation waveform. Note

that as we are combining the data and pilot signals without considering the data bit in the reference signal, E5a, E5b, E5d and E5ab will have ambiguities for the sign of the coherent summation.

Reference signals with the 8-PSK-like method

Table 3 shows the reference signal with the 8-PSK-like tracking method. The parameter iT_s is the quantised sub-carrier phase $k(t)$ and is the output of the look-up-table (called here as the function L) defined in the OS SIS ICD (2008). Again the data ambiguity exists in terms of the E5a or E5b data component. It should be noted that unlike the FIC method, the product signal can not be separated from the sum signal. This reference signal when correlated with $y(t)$, produces a AltBOC(15,10) correlation triangle.

Table 3 Possible reference signals with the 8-PSK-like method

Signal component of interest	Reference baseband signal $s_r(t - \hat{\tau})$
E5	$\exp\left(j\frac{\pi}{4}k(t - \hat{\tau})\right)$ with $k(t) = L(e_{a-I}(t), e_{a-Q}(t), e_{b-I}(t), e_{b-Q}(t), iT_s)$

Issues related to the signal tracking with the different architectures

Each of the reference signals yield an architecture to track the signal listed in the left column of the Tables 1, 2 and 3. It is well known that the tracking performance measured in terms of carrier phase jitter and code phase jitter is directly dependent on the signal strength of the received signal (e.g. Kaplan and Hegarty 2006); the more the signal strength the better the performance. Hence it is wise to combine the different components of the signal in order to extract as much power from the received signal as possible.

The data-bit ambiguity and the non-coherent combination

Because of data bit ambiguity coherent combination is not possible in many cases, indicated with a shaded region in Tables 1, 2 and 3. Note that the only coherent combination possible is the E5a and E5b pilot signal combination which results in the E5 pilot signal combination. In the SBT and FIC methods, the alternate combination (for the data bit flip-over) can be represented by changing the sign of the summation between E5a and E5b

components. On the other hand, for the 8-PSK-like tracking, the alternate combination is not directly possible due to the LUT type of implementation. The classical solution to the data-bit ambiguity, which is the non-coherent combination during the correlation process, does not directly serve the purpose of achieving a better tracking since the phase of the signal is lost during the combination process (the phase information is required as an input to the tracking loop modules so as to provide feedback to the NCO).

Spectrum shape and the SBT method

The E5 signal spectrum is symmetric about the centre frequency 1191.795MHz. However, due to the use of Cosine-AltBOC modulation the energy in the first two E5a and E5b lobes are concentrated away from their centre (and hence they are not symmetric across E5a and E5b centre frequencies). The SBT method uses only the PRN code whose spectrum is symmetric about the centre frequency. This is shown in Fig. 2. Thus the reference signal does not entirely match the received signal during the process of correlation. AltBOC uses a 4-level sub-carrier waveform and also considering the front-end filtering, this mismatch will give negligibly inferior performance to the FIC method. Hence this problem is less severe unlike other BOC modulation schemes.

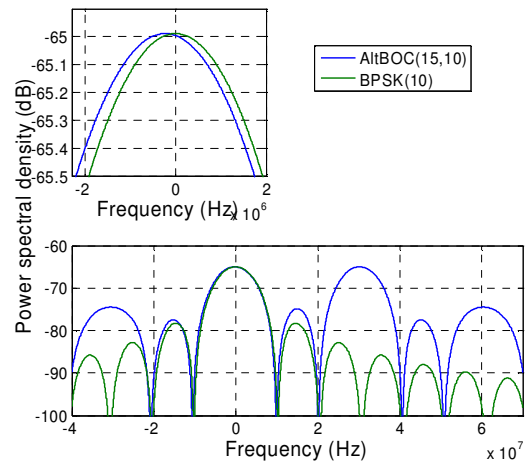


Figure 2 Power spectral density of frequency translated AltBOC(15,10) spectrum and the BPSK(10) spectrum; upper left insert shows the zoom version around the centre.

Carrier tracking, pilot and the data signals

The 8-PSK-like tracking method makes the best use of received signal power, but requires a Costas-loop for the carrier tracking. If we track the E5p component, then it is possible to use a pure phase-locked loop (PLL) to gain a 3dB advantage (Kaplan

and Hegarty 2006) over the E5 signal. The E5p pilot tracking will still be short of 3dB compared to the maximum achievable gain that can be obtained when a combination of E5 signal and a pure PLL is used. On the other hand, the pilot signal tracking can cater for more signal dynamics.

Code tracking linear range

The code tracking linear range directly depends on the sharpness of the underlying correlation function. The E5 signal tracking with the AltBOC(15,10) correlation output has a much sharper main peak compared to the architectures which produce BPSK(10)-like correlation output. On the other

hand, as discussed in previous paragraphs, the 8-PSK-like tracking method gives the best received signal-to-noise ratio among all the architectures. The carrier aiding of the code loop lessens the effect of the code loop dependency, but does not completely eliminate it, especially at lower sampling frequencies. The authors have proposed a novel method of combining the BPSK(10) and AltBOC discriminator outputs to overcome this problem (Shivaramaiah and Dempster 2009).

Table 4 summarises the important discussion issues so far. Later in the paper, performance evaluation results of some of these architectures will be provided.

Table 4 Indicative performance of different tracking architectures

Signal Component	Performance (relative to each other)			
	Code phase jitter	Carrier phase jitter	Code tracking linear range	Power sharing (infinite bandwidth)
E5 8-PSK AltBOC	Very good	Good	Poor	100%
E5a pilot / E5b pilot (with SBT)	Poor	Good	Good	21%
E5a data / E5b data (with SBT)	Poor	Poor	Good	21%
E5a pilot / E5b pilot (with FIC)	Poor	Good	Very good	25%
E5a data / E5b data (with FIC)	Poor	Poor	Very good	25%
E5 pilot (with FIC)	Good	Very Good	Very good	50%
E5 data (with FIC)	Good	Good	Very good	50%
E5ab (with FIC)	Good	Good	Poor	100%

III. HYBRID TRACKING LOOP ARCHITECTURES

A quasi-coherent combination (data wipe-off)

An important requirement of a hybrid architecture is to utilise the received signal power to the maximum extent possible. To achieve this, the complete E5 signal should be used for tracking, and data-bit ambiguity should be avoided. The data-bits in E5a and E5b can be added constructively or destructively. Because of the two data bits, there are four cases and we combine the correlation outputs for these cases. Basically, four correlation outputs $\bar{y}_{0i,l}$, $i=1,2,3,4$, are obtained from the AltBOC LUT from the reference signals:

$$s_{0i}(t - \hat{\tau}) = \exp\left(j\frac{\pi}{4}k_i(t - \hat{\tau})\right),$$

where

$$k_1(t) = L(e_{a-I}(t), e_{a-Q}(t), e_{b-I}(t), e_{b-Q}(t), iT_s),$$

$$k_2(t) = L(e_{a-I}(t), e_{a-Q}(t), -e_{b-I}(t), e_{b-Q}(t), iT_s),$$

$$k_3(t) = L(e_{a-I}(t), -e_{a-Q}(t), e_{b-I}(t), e_{b-Q}(t), iT_s),$$

$$k_4(t) = L(e_{a-I}(t), -e_{a-Q}(t), -e_{b-I}(t), e_{b-Q}(t), iT_s) \quad (6)$$

Note in (6), the negative sign used for the data signal components E5a-I and E5b-I. Also note that $\bar{y}_{0i,l}$ are the complex correlation outputs. Instead of the non-coherent combination, we use the magnitudes of these complex correlation outputs to form the quasi-coherent combination. We formulate:

$$z_{0,l}^{\max} = \max_i(\bar{y}_{0i,l}) \quad (7)$$

The index of iteration l typically corresponds to an integration period of 1 ms, but can be increased up to 4 ms, which is the symbol duration. The index i identifies each of the data/pilot channels from which the maximum correlation value can be directly mapped to obtain the E5a and E5b data bits.

A closely related method called the semi-coherent combination has been discussed to improve the signal-to-noise ratio in the case of GPS L5 signal acquisition (Yang and Hegarty 2004).

Fig. 3 shows the architecture of the data wipe-off method. The output $z_{0,l}$ obtained with the on-time

reference signal is used for the carrier tracking. The combination which maximises the on-time output is also used to select the output of the early and late correlator outputs $z_{1,m}$ and $z_{2,m}$. Observe that we use

two different notations for the integration duration because the code and carrier tracking may have different integration durations.

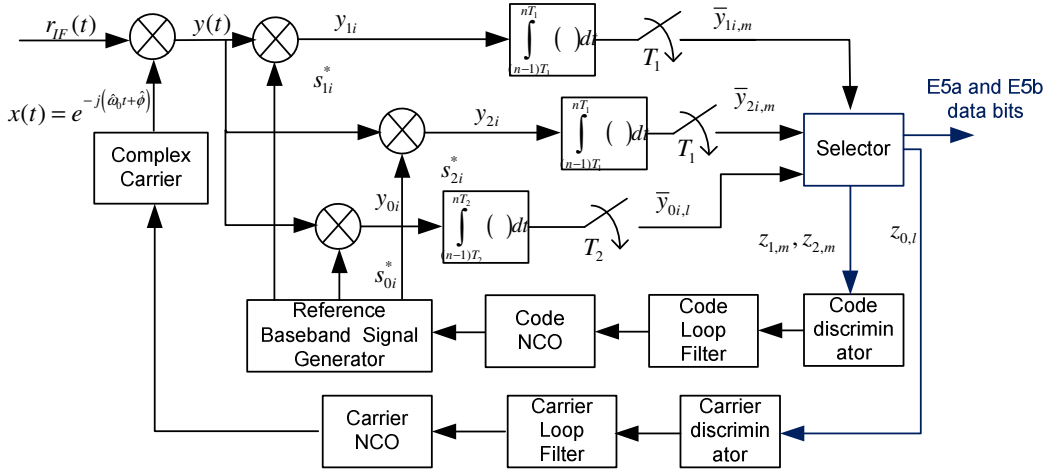


Figure 3 A quasi-coherent (data wipe-off) architecture

This method has a trade-off. Increasing the integration duration for the carrier and code tracking beyond the symbol duration of 4 ms is not straight forward as we would encounter several combinations of the data-bits. This is not a significant problem because the minimum user received power of the E5 signal, -155 dBm (OS SIS ICD, GIOVE-A+B Public SIS ICD 2008) is on the high side compared to other Open Service (or Civilian) signals.

Hardware considerations

The second issue is that of the hardware. If we don't perform the data wipe-off combination, then the tracking loop architecture requires a minimum of 5 complex correlators, three for carrier and code tracking and two for data-bit demodulation. With the data wipe-off architecture we require 12 correlators for a real-time operation (software receivers can buffer the input signal and repeatedly act on it, hence memory and processing time can be traded-off). The good thing is that since the reference signal and the look-up table are already available, a code mixer and an accumulator are the only additions to the hardware. Nevertheless this increases the hardware requirements.

Coherent pilot signal tracking and aiding the data demodulation

Fig. 4 shows the architecture of the coherent pilot tracking method. The reference signal for the carrier and code tracking correspond to the E5p signal component mentioned in Table 2. The X in the Fig. 4 which indicates the reference signal type should

be replaced by E5p to obtain the specific architecture. Since this component is free of data, integration time is only limited by the loop time constant and the signal dynamics that need to be catered for. The data-bits are demodulated using the E5a and E5b components. The reason for using E5a and E5b components instead of E5a-I and E5b-I components is this. Whether it is E5a or E5a-I, the phase change due to the data-bit transition is ± 180 deg because there is only one data component. However, using E5a for the data-bit demodulation provides us with 3dB advantage over the E5a-I. The same argument holds for using the E5b component instead of E5b-I.

Note that the carrier frequency and code delay estimates are used from the pilot tracking and hence no tracking loop is required for the E5a and E5b components. The angles of the complex correlation vales $\bar{y}_{0E5a,m}$ and $\bar{y}_{0E5b,m}$ are mapped to E5a and E5b data-bits correspondingly. The trade-off in this architecture is the received signal power, which is 3dB below the maximum achievable, as explained in section II.

Post-correlation combination methods

The signal components can be combined after the correlation process, at the discriminator stage. These methods have been explored in Hegarty (1999), Tran (2004), Tran and Hegarty (2002) for the GPS L5 and L2C signals. Basically a weighted combination of the discriminator outputs is used as the carrier phase and code delay estimates. These methods can be applied separately to the E5a pilot

and data components denoted here as L(E5a-I, E5a-Q) and to the E5b pilot and data components denoted here as L(E5b-I, E5b-Q). The process of linear combination becomes more difficult in the

presence of two data carrying signals for coherent integrations more than the symbol duration.

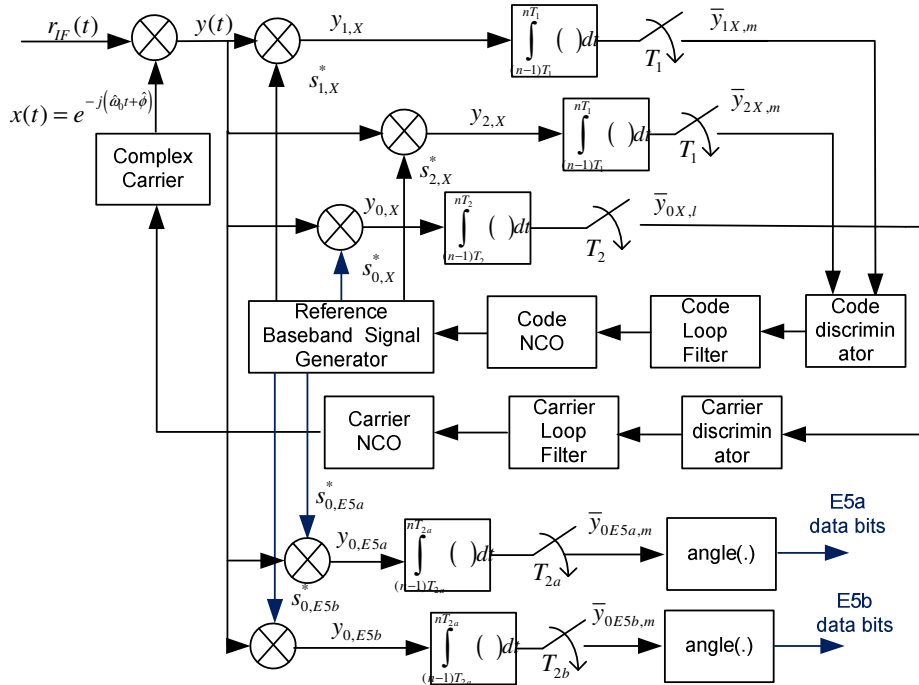


Figure 4 Coherent pilot signal tracking and aiding the data demodulation

Pre-correlation combination architecture

A more efficient way is to look for an architecture which preserves the maximum received signal power without demanding more hardware resources. We propose a pre-correlation combination method in which the local reference signals are added to each other before performing the correlation. Since there are only two possibilities after addition (data bits can be same or data bits can be different) it is sufficient to add two reference signals one corresponding to ‘same sign’ data bit case and the other corresponding to ‘different sign’ data bit case. The same architecture depicted in Fig. 4 can be made use of with the reference signal as in (8). The identifier X has been replaced by PC (Pre-Correlation).

$$s_{0,PC}(t) = \begin{cases} s_{01}(t-\hat{\tau}) + s_{04}(t-\hat{\tau}) & \text{OR} \\ s_{02}(t-\hat{\tau}) + s_{03}(t-\hat{\tau}) \end{cases} \quad (8)$$

Before performing the addition, we need to ensure that the two local signals which we are adding are sufficiently uncorrelated. Fig 5 shows the cross correlation between $s_{01}(t-\hat{\tau})$ & $s_{04}(t-\hat{\tau})$ and $s_{02}(t-\hat{\tau})$ & $s_{03}(t-\hat{\tau})$ for the GIOVE-A code. Observe that the cross correlation is around 18 dB

below zero for both the cases and hence either combination can be used to obtain $s_{0,PC}(t)$.

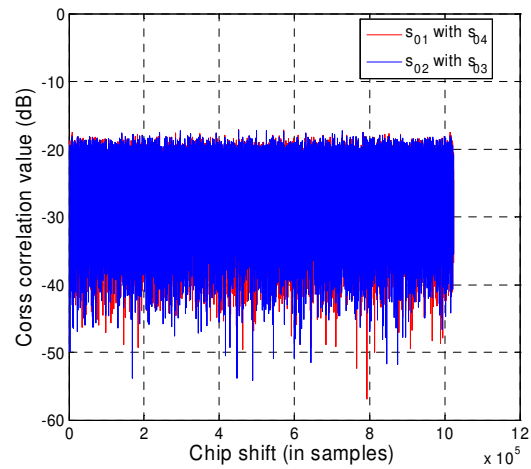


Figure 5 Cross correlation between the different combinations of reference signal (55 MHz front-end bandwidth ;112 MHz sampling);GIOVE-A spreading code

It should be noted that during the addition, there will be an additional noise component and hence the signal-to-noise ratio will be slightly less than that of the data-wipe-off case. We will consider this parameter in the next section while analyzing the performance.

IV. PERFORMANCE ANALYSIS

For the performance analysis, the following receiver design parameters are used. The sampling frequency and the front-end bandwidth are chosen to be 112 MHz and 55MHz respectively, to match the Septentrio GeNeRx1 receiver which was used to collect real signal samples for the bench tests. For the tracking, an early-late chip spacing $d=0.3$, one-sided closed code loop bandwidth B_L of 1 Hz and one-sided closed carrier-lock loop (PLL) bandwidth B_{PLL} of 10 Hz is chosen (stationary receiver tests).

For the carrier tracking, a pure PLL has been used for the pilot components channels and a Costas PLL for the data carrying components. The carrier tracking noise variance is given by (Kaplan and Hegarty 2006):

$$\sigma_{\phi, data}^2 = \frac{B_{PLL}}{a_{data} \cdot C / N_0} \left(1 + \frac{1}{2a_{data} \cdot C / N_0 \cdot T_2} \right) \quad (\text{radians}^2) \quad (8)$$

$$\sigma_{\phi, pilot}^2 \cong \frac{B_{PLL}}{a_{pilot} \cdot C / N_0} \quad (\text{radians}^2) \quad (9)$$

where a_{data} and a_{pilot} are the power sharing factors referenced to the complete E5 signal.

The code tracking noise variance is also analysed for two different discriminator types. The pilot component uses the coherent dot-product type discriminator. It is established in Ries et. al. (2002) that with the BOC family of signals considered, the non-coherent dot-product (DP) type discriminator performs better than the non-coherent early-minus-late-power (NELP) type discriminator. Hence we use the non-coherent DP discriminator for the data carrying signal components. The code tracking jitter for the BPSK and the AltBOC modulation are given by (Ries et.al. 2002) (in chips²):

$$\sigma_{\varepsilon, pilot}^2 = \frac{B_L [1 - R(dT_c)]}{2a_{pilot} \cdot C / N_0 \cdot K^2} \quad (10)$$

$$\sigma_{\varepsilon, data}^2 = \frac{B_L [1 - R(dT_c)]}{2a_{data} \cdot C / N_0 \cdot K^2} \left(1 + \frac{1}{a_{data} \cdot C / N_0 \cdot T_1} \right) \quad (11)$$

where T_c is the chip duration and R is the underlying correlation function. The slope K is unity for the signal components that produce a BPSK(10)-like correlation waveform. For the signal components that produce the AltBOC(15,10) correlation waveform, $K \cong 8.5$.

Fig. 6 shows the carrier phase error for different signal components. The 8-PSK E5 method outperforms all the other signal components. The E5 pilot signal offers better performance than the linear combination of E5 data and pilot components. E5a data signal has poor performance because of the

power sharing as well as the data-bit ambiguity. Fig. 7 shows the code tracking error standard deviation for the signal components in Fig. 6. Again observe that the 8-PSK E5 method offers the best performance among all the other components. The errors in the E5 and E5p components are much less than other components because the underlying correlation waveform is of the AltBOC(15,10) instead of the BPSK(10)-like correlation waveform.

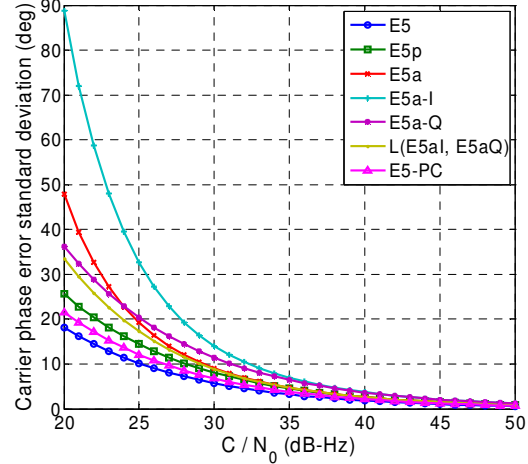


Figure 6 Carrier phase error standard deviation for different signal components

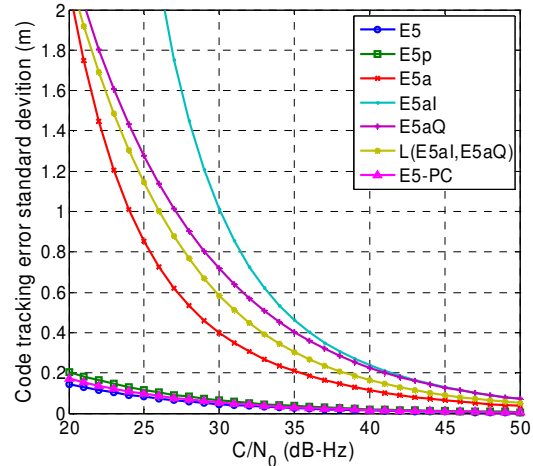


Figure 7 Code tracking error standard deviation for different signal components

Tracking results with the real signal

Using the Septentrio GeNeRx1 receiver, the GIOVE-A satellite signal was collected as digitised intermediate frequency (IF) signal samples during the E5 signal transmission. These data sets were tracked using a MATLAB-based acquisition and tracking module with all the standard architectures as well as the quasi-coherent and E5-pilot tracking architectures, and data-bits were demodulated. Here we provide the tracking results of the quasi-coherent

(data wipe-off) and the pilot signal tracking experiments.

Fig. 8 shows the output of tracking loops for the coherent 8-PSK tracking for the E5 signal without the data-bit wipe-off. Observe that the correlation value drops due to the destructive pattern of the data bits. Fig. 9 shows the prompt correlation outputs for the three types of hybrid tracking methods quasi-coherent 8-PSK, E5 pilot and Pre-correlation combination. Here the reference signals as in (6) and the combination (7) and (8) have been used. Observe that the Pre-correlation method produces slightly noisier output as expected because of two noise components.

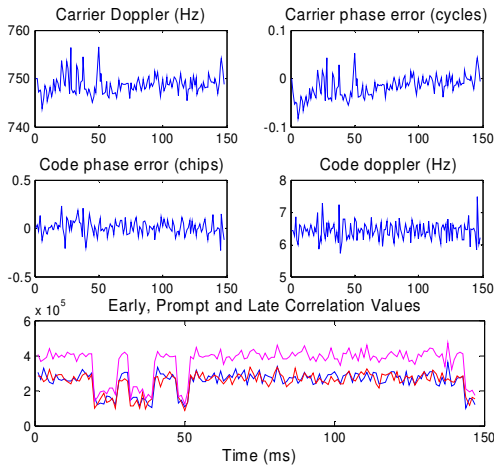


Figure 8 Tracking loop output parameters for coherent 8-PSK tracking of E5 signal : (Dataset-I); Colour Legend: Prompt (magenta), Early (Blue), Late (red)

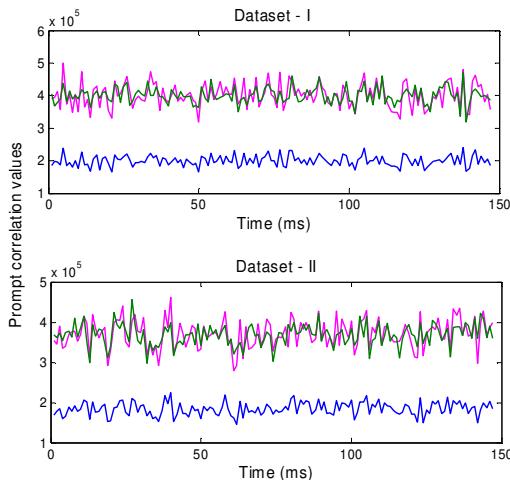
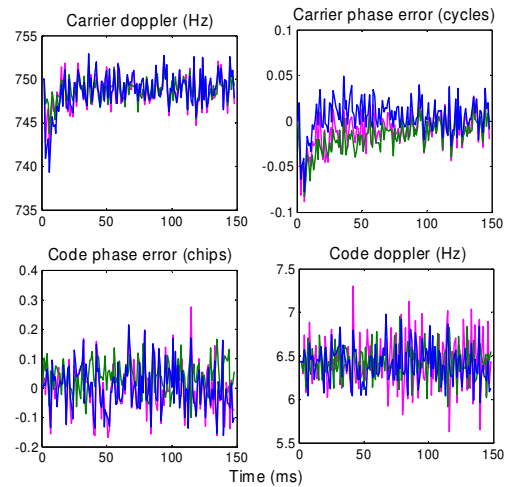


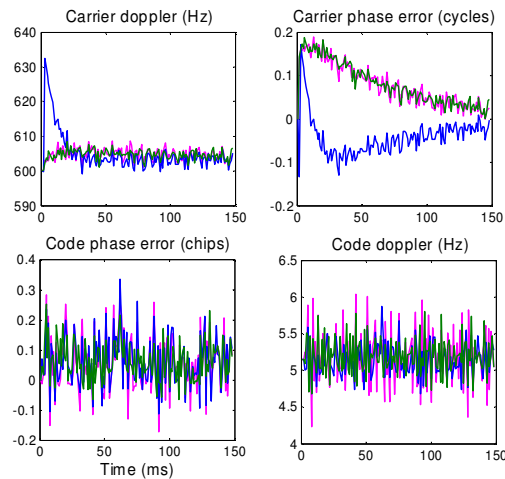
Figure 9 Prompt correlation output for data-bit wipe-off 8-PSK tracking (green); E5 pilot tracking (blue); and Pre-correlation combining method of tracking (magenta)

Fig. 10 shows the tracking loop output parameters for the three types of hybrid tracking methods quasi-

coherent 8-PSK, E5 pilot and Pre-correlation combination. Again observe that the Pre-correlation method produces slightly noisier output compared to the data-bit wipe-off method, but comparable to the E5 pilot tracking method.



(a)



(b)

Figure 10 Tracking loop output parameters for data-bit wipe-off 8-PSK tracking (green); E5 pilot tracking (blue); and Pre-correlation combining method of tracking (magenta); for Dataset-I(a) and Dataset-II (b)

Fig. 11-14 show the correlation values are obtained without any dedicated tracking loops for the E5a and E5b components. Also the phase of the prompt correlation value shown, decodes the data-bit as explained earlier. The datasets were chosen such that the data changes are only in E5b (Dataset-I) and data changes are in both E5a and E5b (Dataset-II). The data bit flip-over are indicated by the 180 deg phase jumps in Figs. 11-14. Colour Legend for Fig. 11-14 (only for Correlation values): Prompt (magenta), Early (Blue), Late (red).

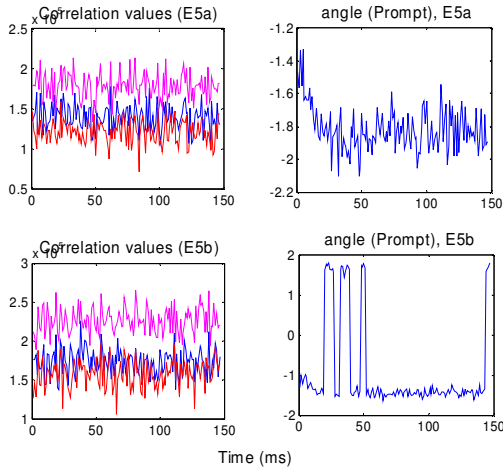


Figure 11 Data-bit demodulation, showing the magnitude and the phase of the correlation values; E5-pilot tracking method: (Dataset-I)

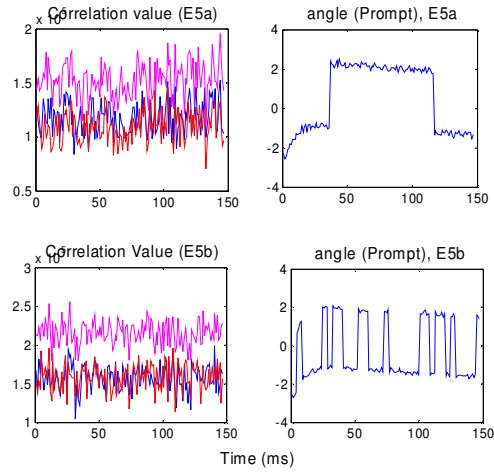


Figure 13 Data-bit demodulation, showing the magnitude and the phase of the correlation values; E5-pilot tracking method: (Dataset-II)

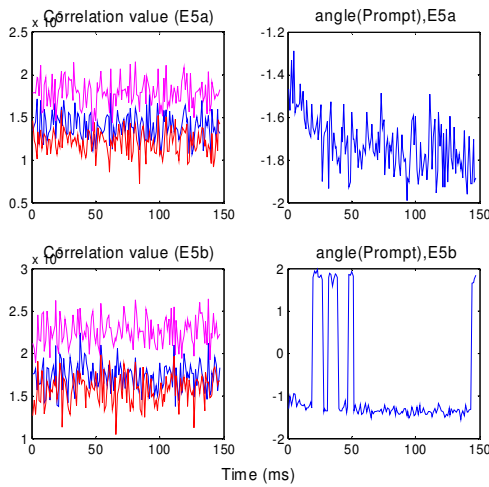


Figure 12 Data-bit demodulation, showing the magnitude and the phase of the correlation values; Pre-correlation combination tracking method: (Dataset-I)

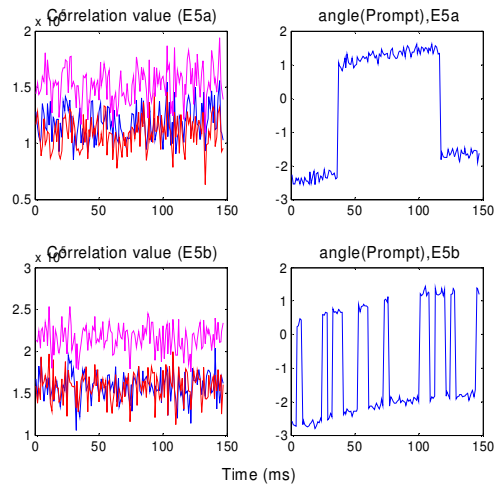


Figure 14 Data-bit demodulation, showing the magnitude and the phase of the correlation values; Pre-correlation combination method: (Dataset-II)

V. CONCLUDING REMARKS

In this paper the authors discussed several tracking architectures that are possible for tracking the E5 signal and its components which make use of different local reference signals. The advantages and disadvantages of the standard tracking architecture are discussed and two types of hybrid tracking architectures are described. Performance of the different tracking loop architectures were analysed, as well as the tracking results of the GIOVE-A E5 signal. It is concluded that the two best architectures are the quasi-coherent 8-PSK tracking for the E5 signal and the E5-pilot tracking. In addition, data demodulation methods were also presented with these two architectures. Further investigation

involves analysing the benefits of interference mitigation with the hybrid tracking architectures.

ACKNOWLEDGEMENT

The authors would like to acknowledge that this research work has been carried out under the Australian Research Council (ARC) Discovery Project DP0556848.

REFERENCES

Sleewaegaen J.-M. et.al. (2004), "Galileo AltBOC Receiver" ENC-GNSS-2004, Rotterdam, The Netherlands, May16-19.

Margaria D. et.al. (2008) “An Innovative Data Demodulation Technique for Galileo AltBOC Receivers”, Journal of Global Positioning System, 2008, vol.6, no.1, 89-96.

Dovis F. et.al. (2007) “Multi-resolution Acquisition Engine Tailored to the Galileo AltBOC Signals”, ION-GNSS-2007, Fort Worth, Texas, USA, Sept 24-28, 999-1007.

Kaplan E.D. and Hegarty C.J. (2006) (Editors) “Understanding GPS: Principles and Applications”, Artech House 2nd Edition.

Hegarty C.J. (1999) “Evaluation of the Proposed Signal Structure for the New Civil GPS Signal at 1176.45 MHz”, Working note WN99W0000034 MITRE document, June 1999.

Tran M. and Hegarty C.J. (2002), “Receiver Algorithms for the New Civil GPS Signals”, ION NTM 2002, San Diego, California, USA, Jan 28-30, 778-789.

Tran M. (2004) ”Performance Evaluation of the New GPS L5 and L2 Civil (L2C) Signals”, Navigation, vol.51, no.3, 199-212.

Shivaramaiah N.C. and Dempster A.G. (2008) “Galileo E5 Signal Acquisition Strategies”, ENC-GNSS-2008, Toulouse, France, Apr 23-25.

Shivaramaiah N.C., Dempster A.G., and Rizos C. (2008) “Exploiting the Secondary Codes to Improve Signal Acquisition Performance in Galileo Receivers”, ION-GNSS-2008, Savannah, Georgia, USA, Sep 16-19, 1497 - 1506.

Soellner M. and Erhard P. (2003) “Comparison of AWGN Code Tracking Accuracy for Alternative-BOC, Complex-LOC and Complex-BOC modulation options in Galileo E5-Band”, ENC-GNSS-2003, Graz, Austria, Apr 22-25.

Ries L. et.al. (2002) “A Software Simulation Tool for GNSS2 BOC Signals Analysis” ION-GPS-2002 Portland, Oregon, USA, Sept 24-27, 2225 - 2239.

OS SIS ICD (2008) Galileo Open Service Signal In Space Interface Control Document, Draft 1, Feb 2008.

GIOVE-A+B Public SIS ICD (2008) Navigation Signal In Space Interface Control Document, Aug 2008.

Yang C., Hegarty C.J., and Tran M. (2004) “Acquisition of the GPS L5 Signal Using Coherent Combining of I5 and Q5”, ION-GNSS-2004, Long Beach, California, USA, Sep 21-24, 2184-2195.

Shivaramaiah N.C. and Dempster A.G. (2009) “A Novel Extended Tracking Range DLL for AltBOC Signals”, Submitted to IEEE VTC FALL 2009.

APPENDIX: ANALYSING THE SIGNIFICANCE OF THE PRODUCT SIGNAL IN GALILEO E5 ALTBOC(15,10)

The product signal is formulated as (using the same notations as the Galileo ICD):

$$E5_{prod} = \frac{1}{2\sqrt{2}} \cdot \left(\begin{matrix} \bar{e}_{a-1}(t-\hat{t})+ \\ j \cdot \bar{e}_{a-Q}(t-\hat{t}) \end{matrix} \right) \cdot sc_{prod}(t-\hat{t}) + \frac{1}{2\sqrt{2}} \cdot \left(\begin{matrix} \bar{e}_{b-1}(t-\hat{t})+ \\ j \cdot \bar{e}_{b-Q}(t-\hat{t}) \end{matrix} \right) \cdot sc_{prod}^*(t-\hat{t}) \quad (6)$$

The product signal has a very interesting feature to play in the total signal, apart from that of helping in producing a constant envelope modulation. The auto-correlation function (ACF) of the product signal for the infinite bandwidth and 70 MHz receiver bandwidth is shown in Fig. A1. Because the correlation function has a very sharp peak, it influences the sharpness of the ACF of AltBOC (15,10). Figs. A2 and A3 show the correlation function of the AltBOC(15,10) signal with and without considering the product component, along with the zoom version around the peak. We can observe that neglecting the product signal yields slightly inferior performances (due to a less sharp main correlation peak) for very high bandwidths. However the same is not true for lower bandwidths.

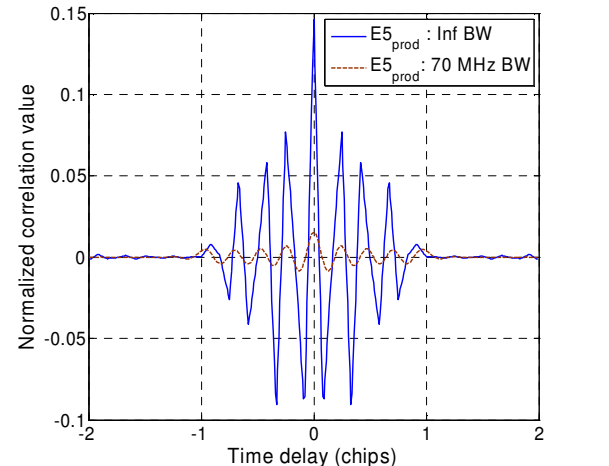


Figure A1 Autocorrelation function of the product signal

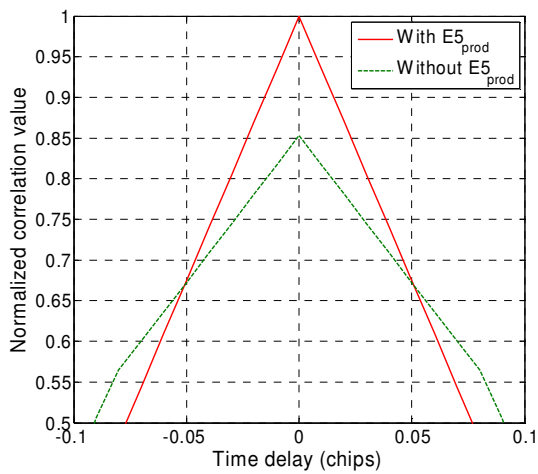
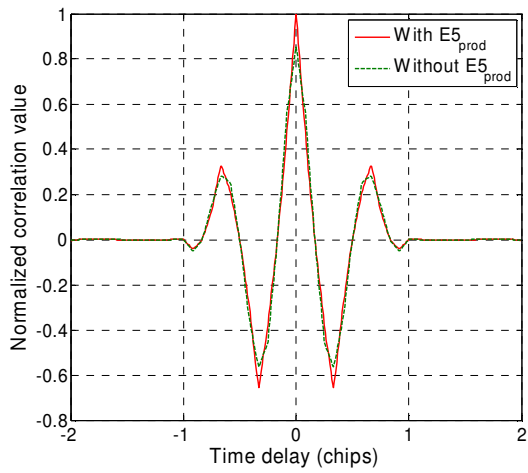


Figure A2 Auto correlation function of the AltBOC(15,10) signal with and without the product signal with infinite bandwidth (top); Zoom version around the peak (bottom).

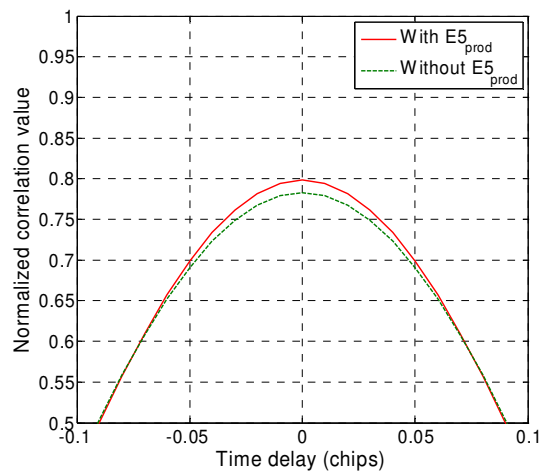
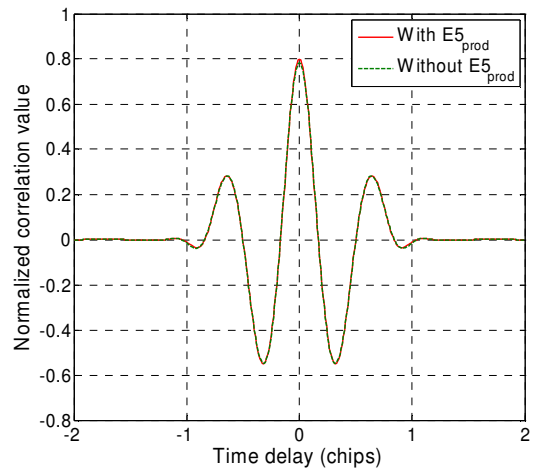


Figure A3 Auto correlation function of the AltBOC(15,10) signal with and without the product signal with 70 MHz bandwidth (top); Zoom version around the peak (bottom).

Because the product sub-carrier frequency is thrice that of the sum-sub-carrier (6 zero crossings as against 2 of the sum sub-carrier), the product signal energy will be concentrated around ± 45 MHz from the centre. Hence a 70 MHz filtering (i.e. ± 35 MHz) will filter out the product signal. Due to this reason, the ACF of AltBOC (15,10) in 70 MHz bandwidth with and without considering the product signal will be very close to each other, as observed in Fig. A3.